

the upper limit on the branching ratio is $R < (28 + 2 \times 57) / 1.1 \times 10^6 = 1.3 \times 10^{-4}$. However, as mentioned above a maximum systematic error of 50% in the yield was estimated as possibly resulting from the comparison of two experiments.¹ Including this possible systematic error results in an upper limit of 2.0×10^{-4} .

This result is approximately an order of magnitude improvement over previous measurements of the muon branching ratio.⁷ The upper limit of the muon branching ratio set by these data is approximately equal to the upper limit on the electron branching ratio of the ρ set by other recent work.⁸ Further work on an improved design of this experiment is now in progress.

We wish to thank the authors of reference 2 and the staff of the Cambridge Electron Accelerator for their aid and cooperation in obtaining data used in this experiment. We wish also to acknowledge the valuable assistance of the research group of reference 1, and most especially of John Russel who provided many experimental details needed to compare the two experiments. One of us (M.G.) acknowledges the many helpful discussions with Dr. von Goeler of Northeastern University concerning this work.

*Work supported in part by the National Science

Foundation under Grants No. NSFG-17419 and No. GP625, and in part by the U. S. Atomic Energy Commission under Contract No. AT(30-1)2098.

†Now at the Stanford Linear Accelerator Center, Stanford University, Stanford, California.

‡Now at Physics Department, Northeastern University, Boston, Massachusetts.

¹L. J. Lanzerotti, R. B. Blumenthal, D. C. Ehn, W. L. Faissler, P. M. Joseph, F. M. Pipkin, J. K. Randolph, J. J. Russel, D. G. Stairs, and J. Tenenbaum, Phys. Rev. Letters **15**, 210 (1965).

²J. K. de Pagter, A. Boyarski, G. Glass, J. I. Friedman, H. W. Kendall, M. Gettner, J. F. Larrabee, and R. Weinstein, Phys. Rev. Letters **12**, 739 (1964). To accept wider angles, the only change necessary in the apparatus was to move the carbon target two feet closer to the iron shielding.

³A complete description of the apparatus, hodoscopes, and recording techniques used will be published soon.

⁴J. D. Bjorken, S. D. Drell, and S. C. Frautschi, Phys. Rev. **112**, 1409 (1958).

⁵H. F. Ehrenberg, R. Hofstadter, V. Meyer-Berkhout, D. G. Ravenhall, and S. F. Sobottka, Phys. Rev. **28**, 214 (1956).

⁶ φ and φ^* refer to the azimuthal angle of the rho and pion pair, respectively.

⁷R. A. Zdanis, L. Madansky, R. W. Kraemer, S. Hertzbach, and R. Strand, Phys. Rev. Letters **14**, 721 (1965).

⁸R. B. Blumenthal, D. C. Ehn, W. L. Faissler, P. M. Josephs, L. J. Lanzerotti, F. M. Pipkin, and D. G. Stairs, Phys. Rev. Letters **14**, 660 (1965).

$\pi^- + p$ ELASTIC SCATTERING FROM 2.5 TO 6 GeV/c*

C. T. Coffin, N. Dikmen, L. Ettlinger, D. Meyer, A. Saulys, K. Terwilliger, and D. Williams

The University of Michigan, Ann Arbor, Michigan

(Received 22 October 1965)

We have measured the differential elastic-scattering cross section for $\pi^- + p$ collisions at four incident pion momenta: 2.5, 3.0, 4.0, and 6.0 GeV/c. The emphasis in this experiment has been placed on scattering at relatively large momentum transfers—in particular, on the structure in the differential cross section near the backward direction and in the region of the secondary maximum at $-t = 1.2$ which has been seen by other experimenters^{1,2} at lower energies.

The experiment was carried out in the 17° beam of the zero-gradient synchrotron (ZGS) at Argonne National Laboratory with the apparatus shown in Fig. 1. A liquid-hydrogen target one foot long and 1.5 inches in diameter is completely surrounded by a coplanar array

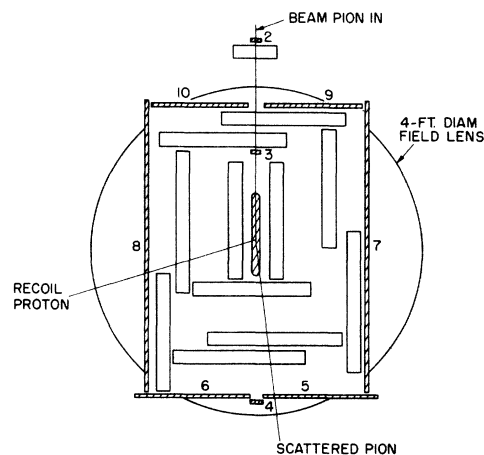


FIG. 1. Plan view of experiment.

of spark chambers and counters. The spark chambers are triggered on a coincidence between any one of the left side counters 6, 8, 10; any one of the right side counters 5, 7, 9; and the beam counters. The size of the side counters was adjusted to maintain nearly constant azimuthal acceptance (around the beam) of about 1/20 for all scattering angles. The beam had an angular divergence of ± 3 mrad and a momentum resolution of $\pm 1\%$.

The film containing the data was first scanned by an automatic flying-spot scanner³ which successfully measures about 90% of the elastic

events. The film was then completely rescanned by human scanners and the remaining events measured on ordinary digital measuring machines. In this way, all candidates for elastic events are reconstructed in space with an angular accuracy of ± 3 mrad.

Event identification was made on the basis of coplanarity of the three tracks and agreement of the scattering angles with elastic-scattering kinematics. These criteria were sufficient to reduce background to approximately 1 $\mu\text{b/sr}$ in the angular region where the cross section is small. The background was always

Table I. $\pi^- + p$ differential cross section (mb/sr).

2.5 GeV/c			3.0 GeV/c			4.0 GeV/c			6.0 GeV/c		
$\cos\theta^*$	$d\sigma/d\Omega$	Error	$\cos\theta^*$	$d\sigma/d\Omega$	Error	$\cos\theta^*$	$d\sigma/d\Omega$	Error	$\cos\theta^*$	$d\sigma/d\Omega$	Error
0.965	10.78	0.28	0.975	12.5	0.3	0.87	0.83	0.06	0.975	10.77	0.32
0.955	8.89	0.26	0.965	10.6	0.3	0.85	0.56	0.04	0.965	7.89	0.28
0.945	7.78	0.23	0.955	8.52	0.25	0.83	0.34	0.03	0.955	5.58	0.23
0.935	6.78	0.22	0.945	7.21	0.22	0.81	0.23	0.03	0.945	3.53	0.18
0.925	5.82	0.20	0.935	6.17	0.20	0.78	0.141	0.017	0.935	2.28	0.15
0.915	5.09	0.18	0.925	5.25	0.19	0.74	0.098	0.014	0.925	1.39	0.12
0.905	4.51	0.18	0.915	4.59	0.18	0.70	0.099	0.014	0.915	1.00	0.10
0.895	4.05	0.17	0.905	3.82	0.16	0.66	0.063	0.012	0.905	0.83	0.09
0.885	3.32	0.15	0.895	2.72	0.14	0.62	0.080	0.013	0.89	0.51	0.05
0.875	2.99	0.14	0.885	2.59	0.14	0.58	0.056	0.012	0.87	0.23	0.03
0.865	2.51	0.13	0.875	2.12	0.12	0.54	0.036	0.008	0.85	0.111	0.025
0.855	2.22	0.12	0.865	1.66	0.11	0.50	0.029	0.006	0.82	0.058	0.012
0.845	1.80	0.11	0.855	1.52	0.10	0.46	0.020	0.005	0.775	0.052	0.011
0.835	1.42	0.10	0.845	1.31	0.10	0.42	0.014	0.005	0.725	0.015	0.006
0.825	1.14	0.08	0.835	1.00	0.09	0.35	0.005	0.002	0.675	0.014	0.006
0.815	1.12	0.08	0.825	0.82	0.08	0.25	0.003	0.002	0.625	0.006	0.004
0.805	0.81	0.07	0.815	0.78	0.07	0.2			0.60		
0.790	0.75	0.05	0.805	0.56	0.06						
0.77	0.52	0.04	0.79	0.43	0.04						
0.75	0.39	0.04	0.77	0.36	0.04						
0.73	0.26	0.03	0.74	0.21	0.02						
0.71	0.15	0.02	0.70	0.142	0.016						
0.65	0.103	0.011	0.66	0.118	0.015	-0.8			-0.9		
0.55	0.117	0.012	0.62	0.106	0.014	-0.85	0.0010	0.0007	-0.942 ^a	0.003	0.002
0.45	0.148	0.015	0.55	0.140	0.014	-0.942 ^a	0.006	0.002			
0.35	0.194	0.017	0.45	0.105	0.011						
0.25	0.163	0.015	0.35	0.074	0.010						
0.15	0.146	0.014	0.25	0.070	0.009						
0.05	0.147	0.015	0.15	0.044	0.007						
-0.05	0.094	0.011	0.05	0.034	0.005						
-0.15	0.050	0.008	-0.05	0.012	0.003						
-0.25	0.016	0.004	-0.15	0.004	0.002						
-0.35	0.009	0.004	-0.25	0.0020	0.001						
-0.45	0.004	0.002	-0.35	0.013	0.003						
-0.55	0.008	0.003	-0.45	0.015	0.003						
-0.65	0.010	0.003	-0.55	0.009	0.003						
-0.75	0.013	0.003	-0.65	0.010	0.003						
-0.85	0.043	0.006	-0.75	0.013	0.003						
-0.942 ^a	0.048	0.006	-0.85	0.008	0.003						
			-0.942 ^a	0.011	0.003						

^aInterval covers -0.900 to -0.985.

negligible in the region of the diffraction peak.

The following corrections were applied to the data:

(1) Azimuthal acceptance factor. This is about a factor of 20 and varies by at most 20% over the whole range of scattering angle.

(2) Absorption and multiple scattering of the recoil protons in the hydrogen and spark chambers. This correction is significant only for the small-angle scattering data in the forward part of the diffraction peak, where it reaches a maximum of 15%.

(3) Muon and electron contamination in the beam. This was determined by absorption studies and Cherenkov counter measurements and was 5% or less for all beam momenta. We believe the absolute normalization to be correct to within about $\pm 5\%$.

Our data are presented in Table I where $d\sigma/d\Omega$ is given as a function of cosine of the center-of-mass scattering angle, θ^* . The differential cross sections for all four momenta have three distinct structural features; the familiar forward diffraction peak, a secondary maximum (or shoulder at higher beam momenta), and a peak in the backward direction at $\cos\theta = -1$. We now discuss the variation of these features with incoming pion momentum.

It has been noted previously^{1,4,5} that in the region of momentum transfer $-t$ from 0 to about 0.7, the differential cross section can be expressed in the form $d\sigma/dt = Ae^{+Bt}$ and that B is nearly independent of incoming pion momentum. At all four momenta we find a value for B of about $7.8 (\text{GeV}/c)^{-2}$ in agreement with the values found at¹ 2.0 and at⁴ 8.5 GeV/c. At 2.5 and 3.0 GeV/c there are small but possibly significant deviations from an exponential shape in the region $t = -0.2$ to -0.5 . These deviations may be associated with the spin-flip amplitude, which is known⁶ to be present in the diffraction region at 2.5 GeV/c, or with resonances.

The variation of the secondary maximum with incoming pion momentum may be seen from Fig. 2 where $d\sigma/dt$ is plotted versus $-t$. We have included for comparison smooth curves drawn through some of the data previously reported at lower^{2,7} and higher⁴ momenta. It is evident that the size of this secondary maximum decreases smoothly with increasing beam momentum from 2.5 to 6.0 GeV/c as a continuation of its behavior at lower energies. The higher energy data at 12.4 and 18.4 GeV/c indicates that the exponential curve characterizing the diffraction peak changes rather sud-

denly at $-t = 0.6$ and at larger momentum transfers is consistent with a smaller slope. Our data at 6.0 GeV/c approach this two-slope exponential dependence. It is interesting to note that there is evidence for secondary maxima in π^+p scattering at¹ 2.0 and at⁸ 4.0 GeV/c similar to those in π^-p scattering at the same momenta. A secondary maximum is also present in charge-exchange scattering between 1.7 and 2.5 GeV/c,⁹ where it is found to shrink with increasing momentum in a way qualitatively similar to that shown in Fig. 2. It then appears that these secondary maxima are a general feature of all pion-nuclear scattering, smoothly shrinking with increasing momentum between 2.5 and about 10 GeV/c. Below 2.5 GeV/c the same effect also seems to be present but its energy variation is not so smooth, perhaps because of interference with the $I = \frac{1}{2}$ resonance at 2.0 GeV/c.¹⁰ The presence of a large polarization^{6,7} throughout the region of the secondary maximum for incident pion momentum between 1.7 and 2.5 GeV/c shows that any meaningful parametrization of this effect must include large real and spin-flip contributions to the scattering amplitude. We have not yet been success-

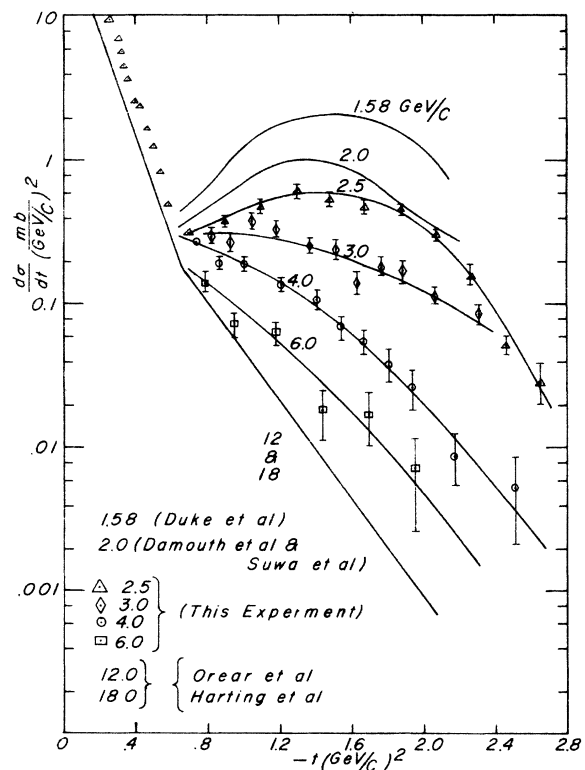


FIG. 2. Momentum dependence of π^+p elastic differential cross section.

ful in finding a suitable parametrization.

In contrast to the behavior of the secondary maxima neither the size nor the shape of the backward peaks in our angular distribution vary smoothly with beam momentum. The peaks at 2.5 and 4.0 GeV/c are relatively sharp, having widths at $\frac{1}{4}$ -maximum of $\Delta \cos\theta^* = 0.24$ and 0.1, respectively, while the peak at 3.0 GeV/c is essentially flat over an interval of $\Delta \cos\theta^* = 0.6$. It may be that resonant amplitudes are important^{11,12} in the region of the backward peak where the cross section is considerably smaller than in the region of the secondary maximum. It is clear that more data at intermediate energies will be required before any definite statement can be made about the cause of the variation in the shape of the backward peak.

We wish to acknowledge the cooperation and support of Dr. L. C. Teng, Dr. Ron Martin, and other members of the staff of the Argonne ZGS. We are grateful to Dr. Vac Sevcik and to Frank Lawrentz for the development and operation of our hydrogen target. We also wish to thank Professor L. W. Jones, Professor M. Longo, and Professor O. Overseth for advice and assistance during the early stages of this experiment.

*Work performed under the auspices of the U. S. Atomic Energy Commission and supported in part by the U. S. Office of Naval Research.

¹D. E. Damouth, L. W. Jones, and M. L. Perl, Phys. Rev. Letters 11, 287 (1963).

²P. J. Duke *et al.*, Phys. Rev. Letters 15, 468 (1965).

³R. Allen, D. I. Meyer, and A. Saulys, to be published.

⁴D. Harting *et al.*, Nuovo Cimento 38, 60 (1965).

⁵M. L. Perl, L. W. Jones, and C. C. Ting, Phys. Rev. 132, 1252 (1963).

⁶Norman E. Booth *et al.*, Proceedings of the International Conference on High Energy Physics, Oxford, 1965 (to be published); also private communications with Akihiko Yokasawa and Norman Booth.

⁷Shigeki Suwa *et al.*, Phys. Rev. Letters 15, 560 (1965).

⁸M. Aderholz *et al.*, Phys. Letters 10, 248 (1964).

⁹A. S. Carroll *et al.*, Proceedings of the International Conference on High Energy Physics, Oxford, 1965 (to be published).

¹⁰A. N. Diddens *et al.*, Phys. Rev. Letters 10, 262 (1963).

¹¹The total energy in the center-of-mass system at laboratory momentum 3.0 is one half-width below that for the $I = \frac{1}{2}$ resonance at 3.24. See A. Citron *et al.*, Phys. Rev. Letters 13, 205 (1964).

¹²The possibility that there is an appreciable interference between resonant and nonresonant amplitudes in this region of laboratory momentum is discussed by R. Heinz and Marc Ross, Phys. Rev. Letters 14, 1091 (1965).